Journal of Organometallic Chemistry 573 (1999) 225–231

Reaction of ruthenium carbonyl chloride with iridium tetracarbonyl anion. Synthesis, crystal structure and characterisation of $[Ru_2Ir_2H(CO)_{12}Cl]$: a heterometallic tetranuclear butterfly cluster with chloride bridge[1]

Aapo U. Härkönen [a], Markku Ahlgrén [a], Tapani A. Pakkanen [a,*], Jouni Pursiainen [b]

[a] *Department of Chemistry, University of Joensuu, PO Box 111, FIN-80101 Joensuu, Finland*
[b] *Department of Chemistry, University of Oulu, Linnanmaa, FIN-90571 Oulu, Finland*

Received 4 April 1998

Abstract

Reaction between $[Ru_2(CO)_6Cl_4]$ and $Na[Ir(CO)_4]$ in tetrahydrofuran (THF) yielded $[Ru_2Ir_2H(CO)_{12}Cl]$, a new iridium–ruthenium mixed-metal cluster of possible catalytic interest. The cluster was characterised by ^1H-NMR and infrared spectroscopy and by single-crystal X-ray structure analysis. $[Ru_2Ir_2H(CO)_{12}Cl]$ exhibits a butterfly arrangement of metal atoms, with three terminal carbonyls on each metal atom, chloride ligand in the bridging position, and hydride ligand at the Ir–Ir edge. The trinuclear ruthenium cluster $[Ru_3(\mu\text{-}Cl)_2(CO)_8(PPhMe_2)_2]$ was synthesised by reaction of $[Ru_2(CO)_6Cl_4]$ with $K[Ir(CO)_4]$ in THF, followed by ligand substitution with $[PPhMe_2]$ in CH_2Cl_2 at ambient temperature. Determination of the structure by X-ray diffraction showed it to consist of an open trinuclear unit involving two metal–metal bonds. The open edge of the metal framework is supported by two symmetric bridging chloride ligands. Both phosphorus ligands are *cis* to the chlorine atoms and *trans* to the unique ruthenium atom. © 1999 Elsevier Science S.A. All rights reserved.

Keywords: Ruthenium; Iridium; Cluster; Carbonyl; Crystal structure; Chlorine

1. Introduction

Although much work has been done on tetranuclear mixed-metal clusters of ruthenium, cobalt and rhodium [1,2], there are only a few reports of closed tetranuclear compounds containing a ruthenium and iridium mixed-metal framework. The synthesis and characterisation of a series of tetranuclear Ru_3Ir and Ru_2Ir_2 clusters have recently been described [3,4], but Ru_2Ir_2 frames are not well known. In the context of our current interest in synthesising and isolating mixed-metal clusters, we have now studied the reaction of $[Ru_2(CO)_6Cl_4]$ with $Na[Ir(CO)_4]$ and $K[Ir(CO)_4]$.

Reaction between $[Ru_2(CO)_6Cl_4]$ and $Na[Ir(CO)_4]$ yielded a new mixed-metal cluster with a Ru_2Ir_2 frame. Characterisation of the cluster by infrared and ^1H-NMR spectroscopy and X-ray diffraction analysis showed it to be $[Ru_2Ir_2H(CO)_{12}Cl]$ (**1**), containing a butterfly arrangement of the metal atoms with chlorine bridging the two ruthenium 'wings'.

Tetranuclear iron [5] and ruthenium [6] clusters are known for forming butterfly structures, including mixed-metal butterfly structures. Very few examples exist, however, of opened tetranuclear butterfly clusters incorporating ruthenium–iridium heterometallic frames. We have previously reported the synthesis and structural characterisation of the chlorine bridged but-

---

* Corresponding author. Fax: +358 13 2513344; e-mail: Tapani.Pakkanen@Joensuu.FI

[1] Dedicated to Professor Brian Johnson on the occasion of his 60th birthday in recognition of his outstanding contributions to organometallic and inorganic chemistry.

PII S0022-328X(98)00703-7

terfly Ru–Ir heterometallic cluster $[Ru_3IrH_2(CO)_{12}Cl]$ [7], in which the chlorine atom is interacting with both transition metals. Other Ru–Ir mixed-metal butterfly structures described in the literature are $[Ru_3Ir(\eta^5\text{-}C_5Me_5)H_4(CO)_9]$ and $[Ru_3Ir(\eta^5\text{-}C_5Me_5)H(CO)_{10}BH_2]$ [8].

Reaction between $[Ru_2(CO)_6Cl_4]$ and $K[Ir(CO)_4]$ in tetrahydrofuran (THF) gave products that were unstable towards chromatographic methods and they were stabilised with $PPhMe_2$ ligand. The products of reaction were the new triruthenium cluster complex $[Ru_3(\mu\text{-}Cl)_2(CO)_8(PPhMe_2)_2]$ (**2**) and the compound $[Ru(CO)_2Cl_2(DMSO)_2]$, which was obtained by decomposition of the starting material $[Ru_2(CO)_6Cl_4]$ through reaction with the DMSO used as solvent. A phosphine-substituted triruthenium cluster structure similar to **2** has been reported earlier [9,10]. Investigation of the structure of **2** by infrared and ^1H-, ^{13}C- and ^{31}P-NMR spectroscopy, elemental analysis and X-ray diffraction analysis showed it to consist of a trinuclear open metal framework with two metal–metal bonds.

2. Results and discussion

2.1. Reaction of $[Ru_2(CO)_6Cl_4]$ with $Na[Ir(CO)_4]$

The reaction of $[Ru_2(CO)_6Cl_4]$ with $Na[Ir(CO)_4]$ in THF at room temperature led to the formation of tetranuclear butterfly cluster $[Ru_2Ir_2H(CO)_{12}Cl]$ (**1**, 21%) and to an unidentified purple compound. The residue that did not elute from the silica column was extracted with THF as a brown solution. Attempts to recrystallise the unidentified purple and brown compounds failed.

2.2. Reaction of $[Ru_2(CO)_6Cl_4]$ with $K[Ir(CO)_4]$ with addition of $PPhMe_2$ ligand

The reaction between $[Ru_2(CO)_6Cl_4]$ and $K[Ir(CO)_4]$ yielded products apparently unstable in chromatographic processing and phosphine ligand was used to stabilise them. $[Ru_2(CO)_6Cl_4]$ and $K[Ir(CO)_4]$ were allowed to react in THF at ambient temperature for 1 h. The residue was dissolved in CH_2Cl_2, and $PPhMe_2$ ligand was added. The reaction led to the formation of $[Ru_3(CO)_{12}]$ and $[Ru_4H_4(CO)_{12}]$, and $[Ru_3(\mu\text{-}Cl)_2(CO)_8(PPhMe_2)_2]$ (**2**) was isolated from the reaction mixture in 11% yield. Contrary to the behaviour of $Na[Ir(CO)_4]$, $K[Ir(CO)_4]$ does not participate in mixed-metal cluster formation in this reaction. The role of the counter ion is an interesting feature which can be used as directing the synthesis. The reaction also yielded an unidentified brown compound.

The residue that did not elute from the silica column was extracted with THF as a brown solution. The compound in the solution was characterised by ^1H-NMR spectroscopy and X-ray structure determination as $[Ru(CO)_2Cl_2(DMSO)_2]$. It is evidently formed by decomposition of the starting material, $[Ru(CO)_3Cl_2]_2$, through reaction with the DMSO which was used as solvent in the synthesis of $K[Ir(CO)_4]$. This compound was first synthesised in 1973, upon carbonylation of *cis*-$[RuCl_2(DMSO)_4]$ [11], and its structure has been described [12]. The ^1H-NMR spectrum of $[Ru(CO)_2Cl_2(DMSO)_2]$ in $CDCl_3$ exhibits the SMe resonance at δ 3.37 ppm.

2.3. Structure of $[Ru_2Ir_2H(CO)_{12}Cl]$ (**1**)

The crystal structure of **1** possesses a butterfly arrangement of four metal atoms with chlorine atom bridging the two ruthenium 'wings'. Iridium atoms are located on the hinge bond of the butterfly structure. The structure is presented in Fig. 1, the bond distances in Table 1, and selected bond angles in Table 2.

The structure of $[Ru_2Ir_2H(CO)_{12}Cl]$ is a wing-tip-bridged 62-electron butterfly cluster with dihedral angle of 93.5°. The value of the dihedral angle is comparable to the values of 89.3 and 96.1° in the Ru_3Ir and Ru_3Co clusters of the butterfly mixed-metal structures $[Ru_3IrH_2(CO)_{12}Cl]$ [7] and $[Ru_3CoH(CO)_{12}(SMe_2)]$ [13]. All these values are typical for wing-tip-bridged 62-electron butterfly clusters [14].

A comparison of the chlorine bridging structures of **1** and $[Ru_3IrH_2(CO)_{12}Cl]$ shows the symmetry of the metal skeletons of **1** and $[Ru_3IrH_2(CO)_{12}Cl]$ to be C_{2v} and C_S, respectively. The higher symmetry in the metal skeleton of **1** is the major factor in the higher molecular symmetry (C_{2v}) of the solid state of this compound. The structure of **1** is similar to $[Ru_3IrH_2(CO)_{12}Cl]$ and possesses a pseudo mirror plane passing through the chloride ligand and the M(1) and M(2) atoms.

The carbonyls in **1** are terminal, as in $[Ru_3IrH_2(CO)_{12}Cl]$, whereas in $[Ru_3CoH(CO)_{12}(SMe_2)]$ the 11 carbonyl ligands are terminally coordinated to the Ru_3Co skeleton with one bridging carbonyl in the hinge Co–Ru bond. Space-filling models [15] show that steric pressure from the hydride ligands results in an opening up of the M–M–CO angles along the Ir(1)–Ir(2) edge. The Ir–Ir–CO angles are more obtuse in **1** (av. 113.1°) than analogues angles in $[Ru_3IrH_2(CO)_{12}Cl]$ (av. 95.5°).

The wing metal–metal bonds in **1** are nearly equal, whereas in $[Ru_3IrH_2(CO)_{12}Cl]$ the Ru–Ru bonds (298.9 pm) are clearly longer than the remaining metal–metal bonds, which implies hydrogen-bridged bonds. For the same reason the hinge Ir–Ir bond in **1** is longer (285.8 pm) than the Ru–Ir hinge bond in $[Ru_3IrH_2(CO)_{12}Cl]$ (272.9 pm). Although there is no direct evidence for the position of the cluster hydride, the position can nevertheless be derived indirectly. Accordingly bond dis-

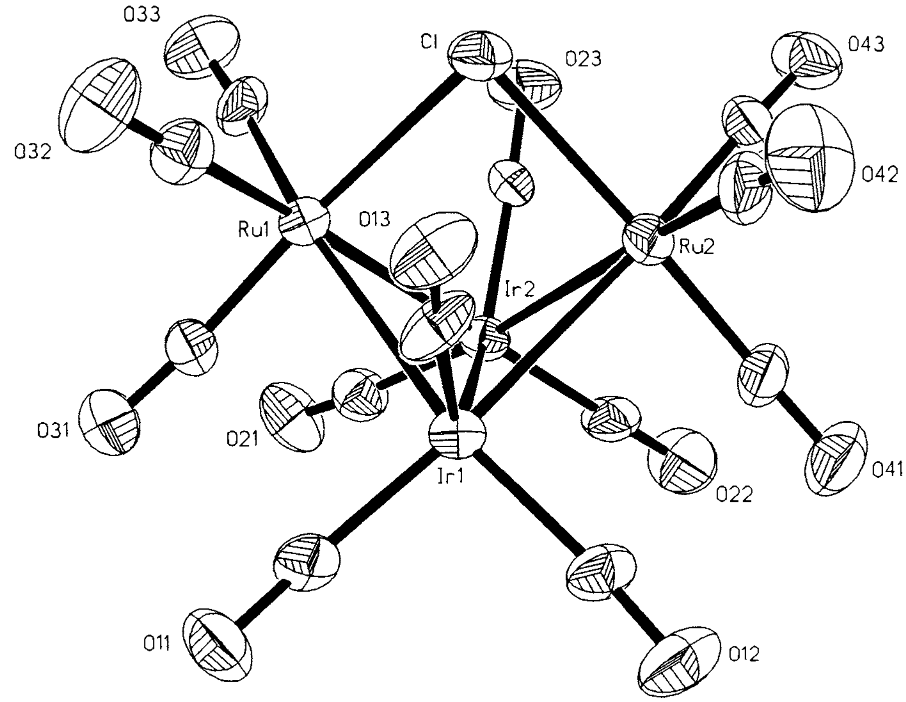

Fig. 1. The molecular structure of $[Ru_2Ir_2H(CO)_{12}Cl]$ (**1**) with the atom labelling scheme. The hydrogen atom μ_2-bonded to the Ir–Ir edge was not located by X-ray methods.

tances the hydride ligand in **1** lies on the Ir(1)–Ir(2) hinge. Also the signal at −19.5 ppm in the NMR spectrum indicates the hydride to be located at the iridium–iridium metal edge. In the Ru(μ_2-H)Ir hydride resonance in $[Ru_3IrH_2(CO)_{12}Cl]$ is at δ −18.7 ppm. The position of the hydride in **1** can be also identified on the basis of the carbonyl conformations.

The Ru(1)–Cl–Ru(2) bridge angle (89.0°) is more acute-angled than the corresponding angles in $[Ru_3IrH_2(CO)_{12}Cl]$ but almost the same as in other halogen-bridged compounds. For example, the metal–halogen–metal bond angles are 88.3° for $[PPN][Ru_4(CO)_{13}Cl]$ [16] and 87.9° for $[Os_4H_3(CO)_{12}I]$ [17].

Table 1
Selected interatomic distances (pm) for $[Ru_2Ir_2H(CO)_{12}Cl]$ (**1**)

Metal–metal			
Ir(1)–Ru(1)	276.7(1)	Ir(2)–Ru(1)	276.2(1)
Ir(1)–Ru(2)	276.5(1)	Ir(2)–Ru(2)	276.5(1)
Ir(1)–Ir(2)	285.8(1)		
Metal–chlorine			
Ru(1)–Cl	246.6(3)	Ru(2)–Cl	245.6(4)
Metal–carbon			
Ir(1)–C(11)	189.0(2)	Ru(1)–C(31)	179.0(2)
Ir(1)–C(12)	192.0(2)	Ru(1)–C(32)	191.0(2)
Ir(1)–C(13)	184.9(1)	Ru(1)–C(33)	188.0(2)
Ir(2)–C(21)	189.0(2)	Ru(2)–C(41)	183.0(2)
Ir(2)–C(22)	191.0(2)	Ru(2)–C(42)	191.0(2)
Ir(2)–C(23)	182.8(1)	Ru(2)–C(43)	186.0(2)

The room temperature ^{1}H-NMR spectrum of $[Ru_2Ir_2H(CO)_{12}Cl]$ in $CDCl_3$ solution exhibits one sharp hydride resonance at δ −19.5 ppm.

2.4. Structure of $[Ru_3(\mu\text{-}Cl)_2(CO)_8(PPhMe_2)_2]$ (2)

The structure of **2** consists of an open trinuclear unit with two metal–metal bonds. The open edge of the metal framework is supported by two symmetric bridging chloride ligands. The phosphorus ligands are coordinated *cis* to the chlorine atoms and *trans* to the unique ruthenium atom Ru(3). The overall geometry of the molecule and the system used for labelling the atoms are presented in Fig. 2. Selected interatomic distances and bond angles are given in Table 3.

Table 2
Selected interatomic angles (°) for $[Ru_2Ir_2H(CO)_{12}Cl]$ (**1**)

Ru(1)–Cl–Ru(2)	89.0(1)		
Cl–Ru(1)–Ir(1)	89.0(1)	Cl–Ru(1)–Ir(2)	88.7(1)
Cl–Ru(2)–Ir(1)	89.3(1)	Cl–Ru(2)–Ir(2)	88.8(1)
C(11)–Ir(1)–Ir(2)	114.4(4)	C(21)–Ir(2)–Ir(1)	112.8(5)
C(12)–Ir(1)–Ir(2)	111.8(5)	C(22)–Ir(2)–Ir(1)	113.4(5)
C(13)–Ir(1)–Ir(2)	127.9(4)	C(23)–Ir(2)–Ir(1)	128.4(4)
C(11)–Ir(1)–Ru(1)	96.2(4)	C(21)–Ir(2)–Ru(1)	91.7(4)
C(12)–Ir(1)–Ru(1)	168.1(5)	C(22)–Ir(2)–Ru(1)	171.4(5)
C(13)–Ir(1)–Ru(1)	80.0(4)	C(23)–Ir(2)–Ru(1)	85.1(4)
C(11)–Ir(1)–Ru(2)	172.3(4)	C(21)–Ir(2)–Ru(2)	168.5(5)
C(12)–Ir(1)–Ru(2)	91.7(5)	C(22)–Ir(2)–Ru(2)	95.5(5)
C(13)–Ir(1)–Ru(2)	83.5(5)	C(23)–Ir(2)–Ru(2)	79.2(4)

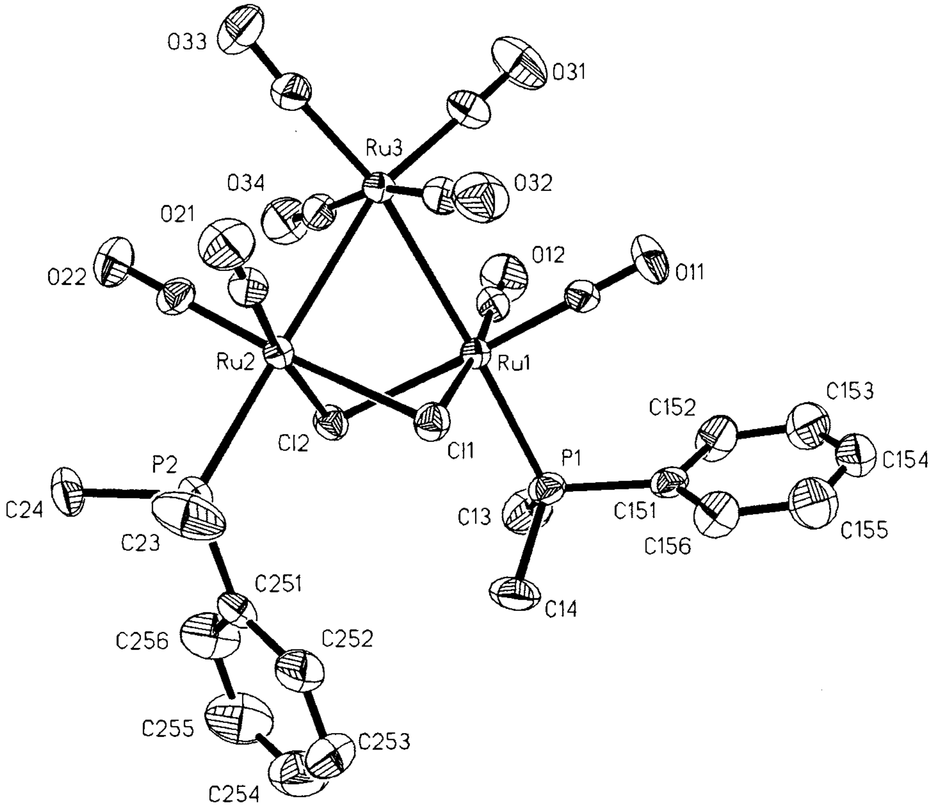

Fig. 2. The molecular structure of $[Ru_3(\mu\text{-}Cl)_2(CO)_8(PPhMe_2)_2]$ (**2**) with the atom labelling scheme. The hydrogen atoms have been omitted for clarity.

The crystal structure of $[Ru_3(\mu\text{-}Cl)_2(CO)_8(PPhMe_2)_2]$ is similar to the structure reported for $[Ru_3(\mu\text{-}Cl)_2(CO)_8(PPh_3)_2]$ [10], which was prepared by pyrolysis of $[Ru_3(\mu\text{-}AuPPh_3)(\mu\text{-}Cl)(CO)_{10}]$. Both structures have approximate C_{2v} symmetry in the crystalline state, and the Ru–Ru bond distances are almost the same: 285.1(1) and 286.0(1) pm for **2** and 284.5(1) and 286.0(1) pm for $[Ru_3(\mu\text{-}Cl)_2(CO)_8(PPh_3)_2]$. The open edge Ru–Ru distance is a little shorter in **2** than in $[Ru_3(\mu\text{-}Cl)_2(CO)_8(PPh_3)_2]$ (318.0(1) pm vs 325.4(1) pm). Other analogous compounds that include two bridge atoms exhibit similar non-bonding distances: viz. $[Ru_3(\mu\text{-}I)_2(CO)_{10}]$ (330.1(1) pm) [18] and $[Ru_3(\mu\text{-}NO)_2(CO)_{10}]$ (315.0(1) pm) [19]. On this basis, it would seem that the non-bonding ruthenium–ruthenium distance is influenced by the size of the bridging atom and the steric hindrance of the ligand.

The ruthenium–chlorine bond distances in **2** are 248.9(1) and 249.4(2) pm for Ru(1)–Cl and 247.7(2) and 249.3(2) pm for Ru(2)–Cl. The chlorine atoms are thus nearly equidistant from the bridged ruthenium atoms. The average Ru–Cl distance, 248.8 pm, is slightly longer in **2** than in $[Ru_3(\mu\text{-}Cl)_2(CO)_8(PPh_3)_2]$ (246.7 pm). Values of the Ru(1)–Cl–Ru(2) angles in the structure of **2** are 79.6(1) and 79.2(1)°.

The distribution of carbonyl ligands in compound **2** is in full agreement with the structural data reported for $[Ru_3(\mu\text{-}Cl)_2(CO)_8(PPh_3)_2]$. Carbonyl groups about Ru(1) and Ru(2) adopt semi-axial positions which are *trans* to the Cl atoms. The Cl–Ru–C values in **2** (average 174.1°) are a little larger than the values in $[Ru_3(\mu\text{-}Cl)_2(CO)_8(PPh_3)_2]$ (average 170.6°). The average value of the Ru–C bonds *trans* to Cl (184.2 pm) is in fair agreement with the structural data for $[Ru_3(\mu\text{-}Cl)_2(CO)_8(PPh_3)_2]$ (181.6 pm). In both cases the metal–carbon bonds are considerably shorter for Ru(1) and Ru(2) than for the unique ruthenium atom: average 192.2 pm for **2** and 190.9 pm for $[Ru_3(\mu\text{-}Cl)_2(CO)_8(PPh_3)_2]$. The clearly shorter Ru–C bond distances are a consequence of the *trans* position of Cl [20].

The phosphine ligands of **2** are bonded *trans* to the Ru(3) atom and lie in almost equatorial sites. Substitution at these specific sites is typical of other analogous clusters [21]. The ^{1}H-NMR spectrum of complex **2** recorded in $CDCl_3$ at room temperature shows resonances at 7.4 and 1.7 ppm, which are the typical resonances for free $PPhMe_2$ ligand in $CDCl_3$. According to the $^{31}P\{^1H\}$-NMR spectrum (signal at −7.2 ppm) recorded under similar conditions, the two phosphine ligands of **2** are equivalent in solution at ambient temperature.

Table 3
Selected interatomic distances (pm) and angles (°) for $[Ru_3(\mu\text{-}Cl)_2(CO)_8(PPhMe_2)_2]$ (**2**)

Ruthenium–ruthenium			
Ru(1)–Ru(3)	285.1(1)	Ru(2)–Ru(3)	286.0(1)
Ru(1)...Ru(2)	318.0(1)		
Ruthenium–chlorine			
Ru(1)–Cl(1)	248.9(1)	Ru(2)–Cl(1)	247.7(2)
Ru(1)–Cl(2)	249.4(2)	Ru(2)–Cl(2)	249.3(2)
Ruthenium–phosphorus			
Ru(1)–P(1)	236.6(2)	Ru(2)–P(2)	238.2(2)
Ruthenium–carbon			
Ru(1)–C(11)	185.5(6)	Ru(3)–C(31)	191.1(6)
Ru(1)–C(12)	183.4(6)	Ru(3)–C(32)	193.5(8)
Ru(2)–C(21)	182.9(7)	Ru(3)–C(33)	191.1(6)
Ru(2)–C(22)	185.0(6)	Ru(3)–C(34)	193.0(8)
Ru(1)–Ru(3)–Ru(2)	67.7(1)		
Ru(1)–Cl(1)–Ru(2)	79.6(1)	Ru(1)–Cl(2)–Ru(2)	79.2(1)
Angles involving Ru(1) atom		Angles involving Ru(2) atom	
Cl(1)–Ru(1)–Ru(3)	88.3(1)	Cl(1)–Ru(2)–Ru(3)	88.4(1)
Cl(2)–Ru(1)–Ru(3)	89.3(1)	Cl(2)–Ru(2)–Ru(3)	89.1(1)
P(1)–Ru(1)–Ru(3)	177.6(1)	P(2)–Ru(2)–Ru(3)	176.5(1)
C(11)–Ru(1)–Ru(3)	87.1(2)	C(21)–Ru(2)–Ru(3)	85.5(2)
C(12)–Ru(1)–Ru(3)	87.6(2)	C(22)–Ru(2)–Ru(3)	86.3(2)
About Ru(3) atom			
C(31)–Ru(3)–Ru(1)	95.2(2)	C(33)–Ru(3)–Ru(2)	98.8(2)
C(32)–Ru(3)–Ru(1)	83.7(2)	C(34)–Ru(3)–Ru(1)	85.1(2)
C(32)–Ru(3)–Ru(2)	84.0(2)	C(34)–Ru(3)–Ru(2)	83.5(2)

3. Conclusions

The reaction of $[Ru_2(CO)_6Cl_4]$ with $[Ir(CO)_4]^-$ in THF was fully characterised and found to give a new tetranuclear mixed-metal cluster and other tetra-, tri- and mononuclear ruthenium complexes. The new cluster, $[Ru_2Ir_2H(CO)_{12}Cl]$, is the first example of a tetranuclear butterfly structure with Ru_2Ir_2 metal frame. In a recent study [7], the Ru_3Ir metal frame was shown to form a wing-tip-bonded butterfly structure as well. In general, tetranuclear clusters with three or four ruthenium atoms form wing tip bonded butterfly clusters. The present work demonstrates an extension of this pattern to tetranuclear clusters with two rutheniums.

Iridium complexes, especially when promoted with ruthenium, have been shown to catalyse carbonylation of methanol [22]. Heterometallic butterfly cluster with Pt_2Ir_2 frame has been found to be active in catalysed homogeneous hydrogenation of olefins [23]. The present work offers a new mixed-metal ruthenium–iridium cluster for catalysis studies, where the metal composition and butterfly structure can be expected to have an influence on the catalytic activity.

4. Experimental details

4.1. General comments

All reactions and manipulations except chromatographic separations were carried out under nitrogen atmosphere using standard Schlenk techniques [24] and with dried and deoxygenated solvents.

Infrared spectra were recorded in *n*-hexane or THF on a Nicolet 20SXC FT–IR spectrometer. ^1H-, ^{13}C- and ^{31}P-NMR spectra were measured on a Bruker AM-250 spectrometer with $CDCl_3$ as solvent at 22°C. The ^1H-NMR spectra were referenced to external Me_4Si, the ^{13}C-NMR spectra to $CDCl_3$, and the ^{31}P-NMR spectra to external concentrated aqueous H_3PO_4. Shifts to higher frequencies relative to the reference were taken as positive. Crystals were grown by evaporation of the solvent from a saturated hexane–CH_2Cl_2 solution.

4.2. Reagents

$[Ru_2(CO)_6Cl_4]$ was of commercial origin (Strem) and was used without further purification. The phosphorus ligand $PPhMe_2$ was purchased from Aldrich Chemical. $K[Ir(CO)_4]$ was prepared from $[IrCl_3]$ by a literature method [25], and $[IrCl_3\ x\ H_2O]$ was of commercial origin (Strem Chemicals). $Na[Ir(CO)_4]$ was prepared from $[Ir_2(CO)_6Cl_2]$ by a literature method [25] and $[Ir_2(CO)_6Cl_2]$ was of commercial origin (Strem).

THF (Merck) was dried and deoxygenated by stirring over Na/benzophenone ketyl, and freshly distilled before use. Other solvents were dried by molecular sieves and deoxygenated by bubbling N_2 through them. KOH was dried in an exsiccator.

4.3. Preparation of [$Ru_2Ir_2H(CO)_{12}Cl$] (**1**)

The compound [$Ru_2(CO)_6Cl_4$] (83 mg, 0.16 mmol) dissolved in 30 ml THF was mixed with a freshly prepared solution of Na[$Ir(CO)_4$] [26] (made from 86 mg, 0.28 mmol [$Ir_2(CO)_6Cl_2$] in THF); the Ir/Ru molar ratio was approximately 1/2. The solution was stirred at room temperature for 3 h. The reddish brown solution was filtered and evaporated in vacuo and the solid residue was treated with 85% H_3PO_4. The residue was extracted with CH_2Cl_2 and gave a red solution. After evaporation of the solvent in vacuo (yielding 314 mg oily solid material), the residue was chromatographed on a silica column (15 cm). Elution of the CH_2Cl_2 extract with hexane gave a yellow band, which was not well eluted. The band was successfully eluted with hexane–dichloromethane (5:1) mixture. Further elution with pure CH_2Cl_2 gave a weak purple band, which did not separate well because the compound decomposed in the column. The yellow fraction was dried in vacuo and was then identified as [$Ru_2Ir_2H(CO)_{12}Cl$] (21 mg, 24%). [$Ru_2Ir_2H(CO)_{12}Cl$] was recrystallised from hexane–dichloromethane at 4°C. Air-stable brown crystals were formed. The infrared spectrum of **1** in *n*-hexane shows bands at 2115w, 2088sh, 2077s, 2071s, 2061s, 2034m, 2022m, 2005w and 1993w cm^{-1} in the carbonyl area. ^{1}H-NMR: -19.5 (s) ppm.

The residue that failed to elute from the column was extracted with THF. A brown solution was obtained, from which the solvent was evaporated in vacuo (yielding 142 mg oily solid material). Attempts to crystallise the brown fraction failed. Its infrared spectrum in THF exhibited ν(CO) absorptions at 2134m, 2128sh, 2066sh, 2058s, 1996m and 1958w cm^{-1}.

4.4. Preparation of [$Ru_3(\mu\text{-}Cl)_2(CO)_8(PPhMe_2)_2$] (**2**)

[$Ir(CO)_4$]$^-$ was extracted with THF from the KOH–DMSO mixture of the K[$Ir(CO)_4$] synthesis (initially 1.008 g, 3.38 mmol [$IrCl_3$ x H_2O]) [25] and the extract was immediately added to a THF solution of [$Ru_2(CO)_6Cl_4$] (366 mg, 0.71 mmol). After stirring at room temperature for 1 h, the solution was evaporated under vacuum and the solid residue was treated with 85% H_3PO_4. The residue was extracted with CH_2Cl_2 and gave a reddish brown solution. A small amount of water was added to the solution to eluted residues of DMSO and the CH_2Cl_2 was evaporated in vacuo (yielding 182 mg solid material).

The solid was dissolved in CH_2Cl_2 (30 ml), and $PPhMe_2$ (12 μl) was added. After 1 h stirring at room temperature the solution was chromatographed on silica column. The majority impurities were removed with hexane, and elution with a 3:1 mixture of hexane–CH_2Cl_2 gave the title compound in 11% yield. Further elution with CH_2Cl_2 gave an unidentified brown fraction. The title compound was crystallised from hexane–dichloromethane at 4°C. IR (CH_2Cl_2): ν(CO) 2075m, 2064w, 2050m, 2038sh, 2023s, 2005m and 1956w. ^{1}H-NMR spectrum ($CDCl_3$): 7.4 (d, C_6H_5, $^2J_{PH} = 6.8$ Hz) and 1.7 (d, CH_3, $^2J_{PH} = 9.4$ Hz) ppm. $^{13}C\{^1H\}$-NMR spectrum ($CDCl_3$): 130.4–129.3 (m, C_6H_5) and 31.6 (s, CH_3) ppm and $^{31}P\{^1H\}$-NMR spectrum ($CDCl_3$): -7.2 ppm. Anal. Calc. for $C_{24}H_{23}Ru_3O_8Cl_2$: C, 32.96; H, 2.54. Found: C, 33.54; H, 2.50.

The residue that did not elute from the silica column was extracted with THF and gave brown solution. The compound was identified as [$Ru(CO)_2Cl_2(DMSO)_2$] by IR and NMR spectroscopy and the identification was confirmed by X-ray diffraction. Air-stable brown crystals of [$Ru(CO)_2Cl_2$-$(DMSO)_2$] were obtained by slow diffusion of hexane/CH_2Cl_2 solution at 4°C. IR data: ν(CO) (CH_2Cl_2) 2084s, 2038sh and 2022vs cm^{-1} and ν(SO) (CH_2Cl_2) 1133m cm^{-1}. The latter signal was attributed to the S–O stretch of an S-bonded Me_2SO ligand. Free Me_2SO absorbs at 1050br cm^{-1}. ^{1}H-NMR: ($CDCl_3$, 293K) δ 3.37 (s, CH_3) and 2.56 (s, free DMSO) ppm.

4.5. Crystallographic summary

Pertinent crystal and refinement data are listed in Table 4. Data were collected on a Nonius Kappa CCD diffractometer for **1** and on a Nicolet R3m diffractometer for **2** using Mo–K_α radiation ($\lambda = 0.71073$ Å). Intensities were corrected for background, polarisation, and Lorentz factors [27] using DENZO and SCALEPACK program package [27] for **1** and SHELXTL program package [28] for **2**. Apart from scaling by SCALEPACK, no absorption correction was applied for **1**. Empirical absorption correction from ψ-scan data for **2** did not improve the result. The relatively high goodness-of-fit for **2** was not found to depend on the weighting scheme.

The metal atom positions were solved by direct methods with use of the SHELXTL program package [28]. All remaining non-hydrogen atoms were located by the usual combination of full-matrix least-squares refinement and difference electron density syntheses using SHELXL93 [29]. Non-hydrogen atoms were refined anisotropically refined for both structures. The hydride atoms were placed in idealised positions (C–H = 0.93 Å, $U = 0.08$ Å^2) and not refined except the hydride ligand in **1** which was excluded since it could not be located from difference maps.

Table 4
Summary of crystallographic data for compounds **1** and **2**

	1	**2**
Empirical formula	$C_{12}HClO_{12}Ru_2Ir_2$	$C_{24}H_{22}Cl_2O_8P_2Ru_3$
Formula weight	959.1	874.5
Crystal system	Orthorhombic	Monoclinic
Space group	$Pna2_1$	$P2_1/n$
a (pm)	1647.2(4)	1403.9(3)
b (pm)	748.6(2)	1213.1(2)
c (pm)	1642.7(4)	1832.6(4)
α (°)	—	—
β (°)	—	91.72(3)
γ (°)	—	—
V (nm^3)	2.0256(9)	3.1196(11)
Z	4	4
$D_{\mathrm{calc.}}$ (g cm^{-3})	3.14	1.88
μ(Mo–K$_\alpha$) (mm^{-1})	15.5	1.72
F(000)	1712	1704
Crystal dimensions (mm)	$0.10\times0.10\times0.15$	$0.15\times0.30\times0.50$
Radiation	Mo–K$_\alpha$	Mo–K$_\alpha$
Monochromator	Graphite	Graphite
Scan range 2θ, (°)	9–53	5–55
Number of reflections collected	18 055	6093
Number of unique reflections	3935	5828
Number of observed data	3673	5471
Number of parameters	262	357
$R[I>2\sigma(I)]$	0.0321	0.0342
$wR(F^2)$[a]	0.0694[b]	0.0605[c]
Goodness of fit	1.009	0.779
Largest difference peak (e nm^{-3})	1008	454
Largest difference hole (e nm^{-3})	-1944	-376

[a] Weight =

$1/[\sigma^2(F_0^2)+(aP)^2+bP]$

where

$P=[(F_0^2)+2F_c^2]/3$.

[b] $a=0.03$ and $b=0.00$.

[c] $a=0.10$ and $b=0.00$.

The positions of all non-H atoms were found by direct methods. Iterative application of least-squares refinement and difference Fourier synthesis led to the solution of the entire structure, including the H atoms. All non-H atoms were refined anisotropically, while the H atoms were freely refined using an isotropic model. Crystallographic calculations were carried out using the SHELXTL-Plus program package [28].

A complete list of bond lengths and angles and tables of thermal parameters and hydrogen atom coordinates has been deposited at the Cambridge Crystallographic Data Centre.

References

[1] B.F.G. Johnson, A. Rodgers, in: D.F. Shriver, H.D. Kaesz, R.D. Adams (Eds.), The Chemistry of Metal Cluster Complexes, VCH Publishers, New York, 1990, p. 317.
[2] T.A. Pakkanen, J. Pursiainen, T. Venäläinen, T.T. Pakkanen, J. Organomet. Chem. 372 (1989) 129.
[3] A.U. Härkönen, M. Ahlgrén, T.A. Pakkanen, J. Pursiainen, Organometallics 16 (1997) 689.
[4] G. Süss-Fink, S. Haak, V. Ferrand, H. Stoeckli-Evans, J. Chem. Soc., Dalton Trans. (1997) 3861.
[5] M. Manassero, M. Sansoni, G. Longoni, J. Chem. Soc., Chem. Commun. (1976) 919.
[6] S. Rossi, J. Pursiainen, T.A. Pakkanen, J. Organomet. Chem. 436 (1992) 55.
[7] A.U. Härkönen, M. Ahlgrén, T.A. Pakkanen, J. Pursiainen, J. Organomet. Chem. 519 (1996) 205.
[8] J.R. Galsworthy, C.E. Housecroft, D.M. Matthews, R. Ostrander, A.L. Rheingold, J. Chem. Soc., Dalton Trans., (1994) 69.
[9] G. Lavigne, F. Papageorgiou, J.-J. Bonnet, Inorg. Chem. 23 (1984) 609.
[10] J.-J. Bonnet, G. Lavigne, F. Papageorgiou, J. Crystallogr. Spectrosc. Res. 16 (1986) 475.
[11] I.P. Evans, A. Spencer, G. Wilkinson, J. Chem. Soc., Dalton Trans. (1973) 204.
[12] E. Alessio, B. Milani, M. Bolle, G. Mestroni, P. Faleschini, F. Todone, S. Geremia, M. Calligaris, Inorg. Chem. 34 (1995) 4722.
[13] S. Rossi, J. Pursiainen, T.A. Pakkanen, Organometallics 10 (1991) 1390.
[14] E. Sappa, A. Tiripicchio, A.J. Carty, G.E. Toogood, in: S.J. Lippard (Ed.), Progress in Inorganic Chemistry, vol. 35, Wiley, New York, 1987, p. 437.
[15] K. Henrick, M. McPartlin, J. Morris, Angew. Chem., Int. Ed. Engl. 25 (1986) 853.
[16] G.R. Steinmetz, A.D. Harley, G.L. Geoffroy, Inorg. Chem. 19 (1980) 2985.
[17] B.F.G. Johnson, J. Lewis, P.R. Raithby, G.M. Sheldrick, K. Wong, M. McPartlin, J. Chem. Soc., Dalton Trans. (1978) 673.
[18] C.E. Kampe, N.M. Boag, C.B. Knobler, H.D. Kaesz, Inorg. Chem. 23 (1984) 1390.
[19] J.R. Norton, J.P. Collman, G. Dolcetti, W.T. Robinson, Inorg. Chem. 11 (1972) 382.
[20] A. Pidcock, R.E. Richards, L.M. Venanzi, J. Chem. Soc. A (1966) 1707.
[21] C.E. Kampe, H.D. Kaesz, Inorg. Chem. 23 (1984) 4646.
[22] C.S. Garland, M.F. Giles, J.G. Sunley, Eur. Pat. App. (to BP), 94306506.0, (1995).
[23] E. Sappa, A. Tiripicchio, A.J. Carty, G.E. Toogood, in: S.J. Lippard (Ed.), Progress in Inorganic Chemistry, vol. 35, Wiley, New York, 1987, p. 514.
[24] D.F. Shriver, M.A. Drezdzon, The Manipulation of Air-Sensitive Compounds, 2nd edn, Wiley, New York, 1986.
[25] L. Garlaschelli, P. Chini, S. Martinengo, Gazz. Chim. Ital. 112 (1982) 285.
[26] M. Angoletta, L. Malatesta, G. Caglio, J. Organomet. Chem. 94 (1975) 99.
[27] Z. Otwinowski, W. Minor, in: C.W. Carter, R.M. Sweet (Eds.), Methods in Enzymology, vol. 276, Academic Press, New York, 1996, pp. 307–326.
[28] G.M. Sheldrick, SHELXTL-Plus; Release 4.11/v, Siemens Analytical X-ray Instruments Inc, Madison, WI, 1990.
[29] G.M. Sheldrick, SHELXL93. Program for the Refinement of Crystal Structures, University of Göttingen, Göttingen, Germany, 1993.